ELSEVIER

Journal of Structural Geology 28 (2006) 943–951

JOURNAL OF STRUCTURAL GEOLOGY

www.elsevier.com/locate/jsg

Influence of measurement errors on stress estimated from single-phase fault/slip data

Yehua Shan [a,*], Ge Lin [b], Zian Li [b], Chongbin Zhao [c]

[a] *Computational Geosciences Research Center, Central South University, Changsha City 410083, P.R. China*
[b] *Guangzhou Institute of Geochemistry, Chinese Academy of Sciences, Guangzhou City 510640, P.R. China*
[c] *CSIRO Division of Exploration and Mining, P.O. Box 1130, Bentley, WA 6102, Australia*

Abstract

The influence of measurement errors on estimated stress is investigated in reduced sigma space on the basis of numerous sets of homogeneous fault/slip data generated under different extensional stress and then modified by varying measurement errors for the striation pitch. For a given measurement error, error propagation to a datum vector depends upon the controlling stress and fault orientation with respect to the controlling stress. For a given stress ratio, both the dispersion of datum vectors (i.e. root mean square cosine) and the misfit between estimated and controlling stresses (i.e. similarity and stress difference) increase with the increase in measurement error. The two measures appear generally smaller at small measurement error than at large error and have a strong tendency to increase with stress ratio for a given measurement error. The measurement error has an apparent effect in estimated stress only if it is greater than 10°, implying a limited effect on homogeneous fault slip data that is carefully measured at outcrop, in which a smaller error can be guaranteed in a majority of cases.

Keywords: Measurement error; Influence; Fault/slip data; Stress inversion; Reduced sigma space

1. Introduction

Faults are widely used to estimate stress in deformed rocks, thereby becoming an important stress gauge for structural geologists. The technique of stress inversion has received much attention recently (Ramsay and Lisle, 2000). A variety of inversion methods have been developed (e.g. Angelier, 1979, 1994; Etchecopar et al., 1981; Armijo et al., 1982; Simón-Gómez, 1986; Huang, 1988; Kleinspehn et al., 1989; Fleischmann and Nemcok, 1991; Hardcastle and Hills, 1991; Nemcok and Lisle, 1995; Nemcok et al., 1999; Yamaji, 2000; Lisle et al., 2001; Shan et al., 2003, 2004a,b,c; Xu, 2004). They differ in algorithms designed to solve for stress. Some of the techniques deal with single-phase (or homogeneous) fault/slip data and others enable analysis of multiple-phase (or heterogeneous) fault/slip data. The principal stress orientations and stress ratio can be estimated by the inversion methods. For a given set of fault/slip data, the misfit between estimated and real stresses may depend upon the inversion method, the heterogeneity (or multiple phases) of the fault/slip data, deviation from the assumptions, measurement errors and so forth.

When fault/slip data are heterogeneous, none of the methods for homogeneous data can be used properly, giving rise to meaningless estimates. In this case, a crucial task is the separation of data into many homogeneous groups before stress inversion. Existing inversion methods (e.g. Hardcastle and Hills, 1991; Nemcok et al., 1999; Yamaji, 2000; Shan et al., 2003, 2004c) developed for this task differ in the theory of data separation and are likely to produce variable results for a given data set (Liesa and Lisle, 2004). Meanwhile, an old clustering problem re-emerges: What is the optimal number of groups we need to make among the data? For the answer, we may turn either to field observations about relative ages of fault formation or reactivation, or to the data themselves in some elaborate way (e.g. Shan et al., 2004c).

There are two fundamental assumptions for stress inversion: homogeneous stress field in a single phase of deformation, and parallelism between the fault striation and the maximum resolved shear in the fault plane from which any departure would lead to deviation of the estimated stress from the controlling (real) stress. Violation of either or both assumptions could be due to reasons such as intermittent

* Corresponding author. Tel.: +86 731 8877077; fax: +86 731 8879602.
E-mail address: shanyehua@yahoo.com.cn (Y. Shan).

0191-8141/$ - see front matter © 2006 Elsevier Ltd. All rights reserved.
doi:10.1016/j.jsg.2006.03.025

fault slip, asynchronous slip along the fault (e.g. Price, 1988; Gutscher et al., 1996), heterogeneous distributions of earthquake shear stress drop over a large area of the rupture surface (e.g. Day et al., 1998) and heterogeneous stress distributions in structurally complex areas (e.g. Mitra, 1987; Koyi, 1995). In reality, some or all of these reasons are inevitable. They can lead to dispersion in the parameter space of measured fault/slip data, or even possibly the presence of superficially heterogeneous fault/slip data. For the latter, we have meaningless data groups and false estimated stresses through conventional inversion methods. This is indeed the Achilles' heel of stress inversion.

Furthermore, errors are inevitable while one measures the orientations of geological features, such as faults or striations, at outcrop with a compass. Measurement accuracy depends upon the precision of compass readings, the exposure quality, experience, skill and carefulness of the person making the measurements and so forth. The larger the measurement errors, the more dispersed the data tend to be and the more incorrect the estimated stress will be.

Heterogeneity (or multiple phases) of fault/slip data, deviation from the assumptions, and measurement errors appear naturally combined with each other in data sets from multi-deformed regions. It is almost impossible to evaluate these factors, because of the difficulty in quantifying them and because of little or no knowledge about the controlling stress. This in turn decreases the reliability of estimated stress. We are interested here in particular questions about measurement error. For example, in the reduced sigma space of Fry (1999), how much misfit is there between datum vectors with and without a measurement error? How does the measurement error affect estimated stress? These questions can be answered without taking the possibility of multiple phases of fault slip into account, as will be shown below.

The aim of this paper is to investigate the influence of measurement errors on estimated stress in reduced sigma space, although it has been addressed before in the other parameter space (e.g. Angelier, 1984; Xu, 2004). For simplicity, only single-phase (homogeneous) fault/slip data were considered in this paper. Although we believe the answers might shed light on the cases of multiple (heterogeneous) fault/slip data, we have intentionally avoided their complexity.

2. Inversion in the sigma space

Although it has a seemingly non-linear character, stress inversion becomes linear in the most part after some transformation. In reduced sigma space (Fry, 1999), fault/slip data were transformed into datum vectors that, if homogeneous, tend to lie in or near a hyperplane (a higher dimension analogue of a 2D plane in 3D space) across the origin. This linearity facilitates the inversion of stress in terms of the use of sophisticated algorithms, some of which are even effective in processing heterogeneous data (Shan et al., 2003, 2004c).

A fundamental assumption of stress inversion is the parallelism between the fault striation and the maximum resolved shear in the fault plane (Angelier, 1979):

$$n\sigma s^{\mathrm{T}} = 0 \tag{1}$$

where $\boldsymbol{\sigma}$ is the unknown controlling stress tensor, $\boldsymbol{n}$ is the unit vector normal to the fault plane, $\boldsymbol{s}$ is the directional vector perpendicular to the fault striation in the fault plane and the superscript T is the operation of matrix transposition.

Let $\boldsymbol{n}=[n_1, n_2, n_3]$ and $\boldsymbol{s}=[s_1, s_2, s_3]$. Rewriting Eq. (1):

$$\sum_{i=1}^{3}\sum_{j=1}^{3} c_{ij}\sigma_{ij} = 0 \tag{2}$$

where $c_{ij}=n_i s_j$. Because of the nine elements of stress tensor, the full sigma space has a dimension of 9. It can be reduced in dimension from 9 to 5 by considering the symmetry of stress tensor and by using some auxiliary constraint below (Fry, 2001):

$$\sum_{i=1}^{3} \sigma_{ii} = 0 \tag{3}$$

Solving σ_{11} from Eq. (3) and inserting the result into Eq. (2):

$$bt^{\mathrm{T}} = 0 \tag{4}$$

where the datum vector $\boldsymbol{b}=[c_{22}-c_{11}, c_{33}-c_{11}, c_{12}+c_{21}, c_{13}+c_{31}, c_{23}+c_{32}]$, and the stress vector $\boldsymbol{t}=[\sigma_{22}, \sigma_{33}, \sigma_{12}, \sigma_{13}, \sigma_{23}]$ (Shan et al., 2003).

Geometrically, in reduced sigma space, the stress vector is perpendicular to the datum vector, as in Eq. (4). The perpendicularity, as well as another constraint of the unit length of the stress vector, guarantees that homogeneous datum vectors prefer to lie in or near a hyperplane across the origin of the sigma space (Fry, 1999). Normal to the hyperplane is the optimal stress vector. However, in relation to $\boldsymbol{t}$, $-\boldsymbol{t}$ is also a solution of stress vector. All the data, as assumed homogeneous, indicate either $\boldsymbol{t}$ or $-\boldsymbol{t}$. The correct identification between them requires the use of fault slip senses (Shan et al., 2004a).

3. Error propagation to datum vectors

Our first interest is to consider the misfit between the datum vectors in reduced sigma space with and without a measurement error, namely, the propagation of measurement errors to datum vectors. For a certain given error, the misfit depends not only upon fault orientations with respect to the controlling stress but also stress ratio.

For each individual fault/slip datum, measurement errors exist not only in the dip direction and dip angle of the fault plane, but also in the bearing and plunge of the fault striation, or in the pitch. In order to describe the measurement error of fault/slip data, we need to consider three errors associated with (i) the fault dip direction, (ii) the fault dip angle, and (iii) the striation pitch. However, these kinds of errors are not independent, because the fault striation lies in the fault plane. The first two errors and the third error are dependent upon each other. Once measurement errors are directly added to a certain fault/slip datum, the new datum must be adjusted in some way to accommodate compatibility among its dip direction, dip angle and plunge.

3.1. Procedure

In this study, for the sake of simplicity, only the error for the pitch was taken into account. This made for convenience in our discussion below, by virtue of a smaller number of variables under consideration. A measurement error is herein defined as positive if the adjusted plunge is larger than the original one, or as negative if smaller. An exception to this definition is where the fault striation is parallel to the down-dip line in the fault plane. However, in this case, the sign of measurement error has no influence on the deviation of the datum vector.

In the light of an infinite number of stresses in nature, our discussion was confined to two controlling stresses with the same principal orientations but different stress ratios. Each stress represents an Andersonian state for the extensional regime, in which the maximum (σ_1), intermediate (σ_2), and minimum (σ_3) principal stresses are directed upwards, northwards and eastwards (Fig. 1a). They have the same directions as the *Z*-axis, the *X*-axis and the *Y*-axis, respectively, in the Cartesian system. The corresponding stress ratios, defined as $(\sigma_2-\sigma_3)/(\sigma_1-\sigma_3)$, are 0.25 and 0.75 for the two controlling stresses. Four different measurement errors for the striation pitch, namely $-8°$, $-4°$, $4°$ and $8°$, are equally added to fault/slip data produced under a given stress tensor. Although it is not difficult to consider other stresses differing from our two controlling stresses, either in stress ratio or in principal directions or in their combinations, and/or other measurement errors, we leave that to interested readers in the interest of brevity.

The procedure used to investigate the effects of measurement errors can be described as follows:

(1) Assign values to the controlling stress and measurement error.

(2) Take the orientation of each fault surface from a 360×90 integer set, namely [0°, 359°] for the fault dip direction, and [1°, 89°] for the fault dip angle, in a sequential manner, and then:

  (a) determine the attitude of the striation in the fault plane under the prescribed stress,
  (b) determine the attitude of the striation with the assigned measurement error, and
  (c) calculate the misfit in angle between the two datum vectors in reduced sigma space with and without the measurement error.

3.2. Results

Results are shown in Figs. 1 and 2 and Table 1, from which several conclusions can be drawn and summarized below:

(1) The misfit between datum vectors with and without a measurement error appears to have an upper limit of a little larger than the value of the measurement error and a lower limit of roughly half of the error (Table 1). This indicates that the misfit is approximately of the same order of magnitude as the measurement error itself.
(2) The misfit between datum vectors with and without a measurement error reaches a minimum where the fault dip direction is parallel to the intermediate principal stress and has a dip angle of ca. 45°. For a stress ratio of 0.25, two maxima exist where the fault dip direction is parallel to the minimum principal stress and has a dip angle of about 45°. In contrast, for a stress ratio of 0.75, there are four maxima, close to each of the two minima, where the fault has a dip of about 60°.
(3) For a given controlling stress, the sign of the measurement error has a very slight influence on the deviation of datum vector caused by the error itself. There is a little difference in the deviation of datum vectors whether the error sign is positive or negative.

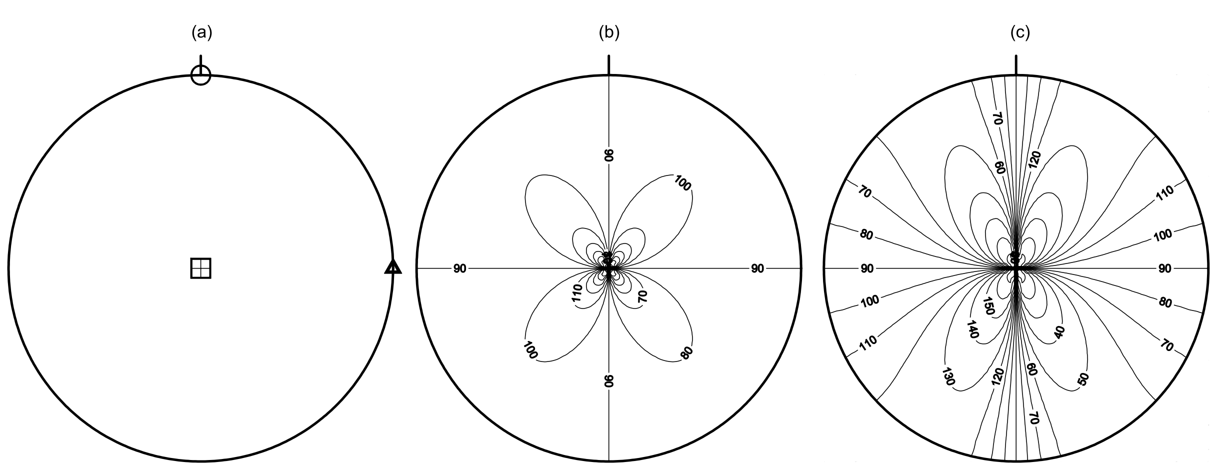

Fig. 1. Prescribed principal directions (a) and contours of striation pitches in angle for a stress ratio of 0.25 (b) and of 0.75 (c). Equal-area, lower hemispheric projection. The maximum, intermediate and minimum principal stress directions are represented by the square, the circle and the triangle, respectively.

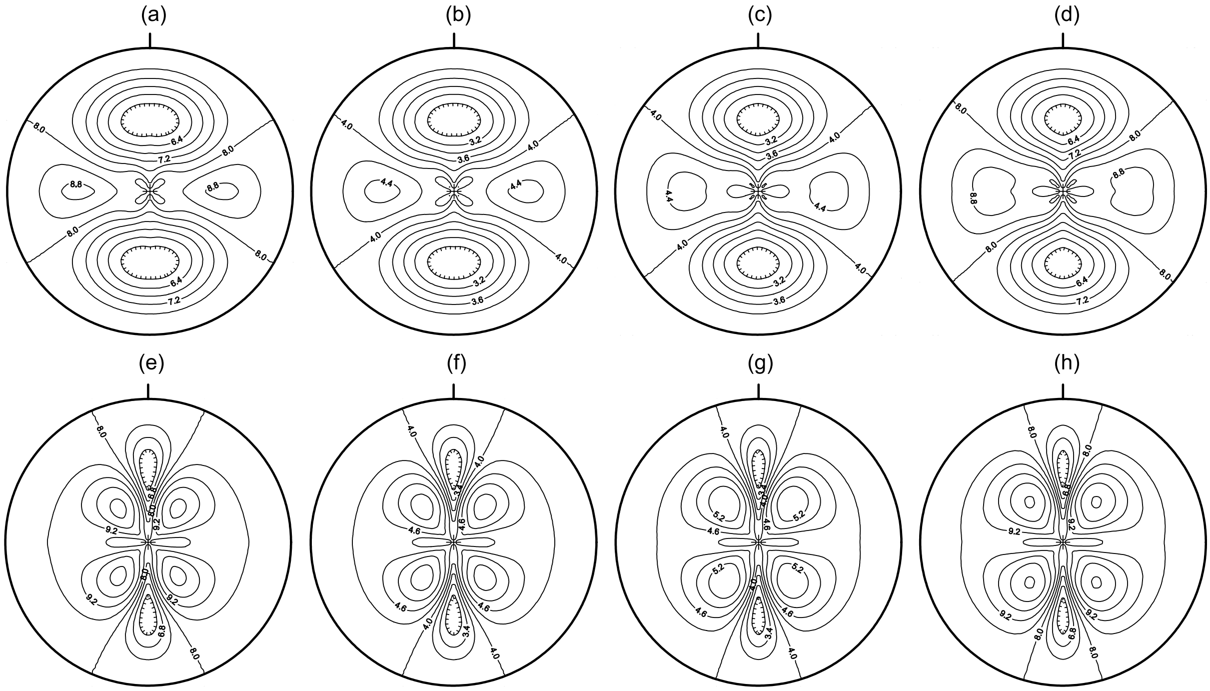

Fig. 2. Contours of the angular misfit in angle between datum vectors without and with measurement errors of 8° ((a) and (e)), 4° ((b) and (f)), −4° ((c) and (g)) and −8° ((d) and (h)). Equal-area, lower hemispheric projection. (a)–(d) are for a stress ratio of 0.25 and (e)–(h) for a stress ratio of 0.75. The hachured contours have the least levels. See the text for more explanation.

4. Influence of measurement error on estimated stress

Normally, measurement errors exist in any fault/slip data measured at outcrop. So, in reduced sigma space datum vectors become dispersed with respect to the hyperplane normal to the vector of the controlling stress. This would lead to the deviation of estimated stress through applying the method of Shan et al. (2003) to these data, from the controlling stress. Also, the deviation depends upon both measurement errors and fault orientations with respect to the controlling stress.

4.1. Definitions of parameters

Despite other possible indicators, root mean square cosine (Shan and Fry, 2005) is used to measure the dispersion of datum vectors in the reduced sigma space, while the intersecting angle and similarity are used to compare the controlling and the estimated stress vectors. In addition, stress difference (Orife and Lisle, 2004) is used to describe the misfit between the controlling and the estimated stresses.

4.1.1. Root mean square cosine

In order to solve for stress vector in the reduced sigma space, an objective function is defined as the sum of squares of distances of individual datum vectors to the unknown hyperplane (Shan et al., 2003). The solution of the expected stress vector is obtained when the objective function reaches the minimum value (E):

$$E = \sum_{i=1}^{n} \left(b_i t'^{\mathrm{T}} \right)^2 \qquad (5)$$

where n is the number of fault/slip data, $\boldsymbol{b_i}$ is the ith datum vector and $\boldsymbol{t}'$ is the best solution of stress vector. The multiplication of $\boldsymbol{b}_i$ and $\boldsymbol{t}'$ equals their distance, because all datum vectors and the stress vector have a unit length, as required before.

The root mean square cosine (R) is defined as follows (Shan and Fry, 2005):

$$R = \sqrt{\frac{E}{n}} \qquad (6)$$

The parameter reflects the mean deviation of datum vectors from the hyperplane, normal to which is the estimated stress vector. There is no definite relation between the dispersion of

Table 1
Statistics of misfit between datum vectors with and without measurement error under varying stress ratio

Stress ratio	Measurement error (°)	Misfit in angle (°)		
		Maximum	Minimum	Average
0.25	−8	8.974	5.675	7.893
	−4	4.473	2.827	3.913
	4	4.470	2.829	3.851
	8	8.30	5.658	7.643
0.75	−8	11.073	5.675	8.872
	−4	5.487	2.831	4.411
	4	5.365	2.831	4.351
	8	10.591	5.662	8.637

data and the accuracy of stress estimation, but the more dispersed the data, the more likely the estimated stress is to be inaccurate.

4.1.2. Intersecting angle and similarity

As stated before, another auxiliary constraint for stress inversion is the unit length of stress vectors (Fry, 1999; Shan et al., 2003). Let t_{est} and t_{con} stand for estimated and controlled stress vectors, respectively. The intersecting angle (θ) and similarity (γ) between the two vectors are defined as:

$$\gamma = t_{est} t_{con}^{T} \quad (7)$$

$$\theta = \arccos(\gamma) \quad (8)$$

4.1.3. Stress difference

Let λ_1, λ_2 and λ_3 be the maximum, intermediate and minimum eigenvalues of the difference matrix between the normalized estimated stress tensor and the normalized controlling stress tensor. The stress difference (D) between the two stress tensors is calculated in the following way (Orife and Lisle, 2003):

$$D = \frac{\sqrt{(\lambda_1 - \lambda_2)^2 + (\lambda_2 - \lambda_3)^2 + (\lambda_1 - \lambda_3)^2}}{3} \quad (9)$$

D has a range of 0–2. It equals 0 when the two tensors are identical and 2 when one is the negative of the other. According to the statistical study of Orife and Lisle (2003), stress tensors are considered very similar if $D < 0.66$, similar if $0.66 < D < 1.01$, different if $1.01 < D < 1.71$, or very different if $D > 1.71$.

4.2. Procedure

In this section, the measurement error sign is allowed to vary as a variable, so that some random nature of the measure error can be considered. For a certain measurement error, there are two options to incorporate it into a fault/slip datum by either increasing or decreasing the striation's pitch by the same angle. We have a number of 2^n different options for a set of n fault/slip data. Therefore, the computing time we take in addressing every possibility increases exponentially with data number n. Even for a small data number, 30 for example, the time becomes too large to do with a personal computer. Sensibly, we had better have a small value of n, 10 in this study for instance, which must be larger than 4, the minimum for stress inversion in reduced sigma space (Fry, 1999). A set of 10 fault data (Fig. 3), including dip directions and dip angles, were generated in a random manner. They were utilized as a template to determine the attitudes of fault striations in the fault planes for different stress ratios.

For a parallel study to the one in the previous section, the Andersonian stress state for the extensional regime was also considered, and so are the prescribed principal directions (Fig. 3) and the Cartesian coordinates. The stress ratios considered are 0.0, 0.25, 0.50, 0.75 and 1.00. Measurement errors were added to fault pitches as integer numbers from 0° to 20°.

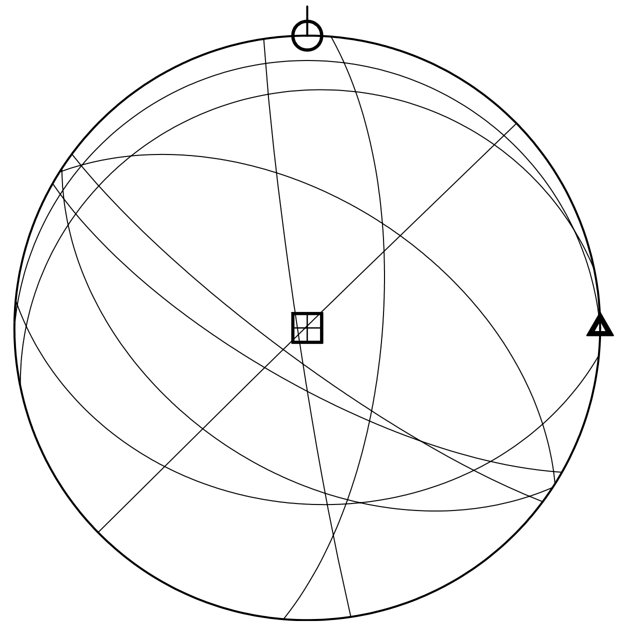

Fig. 3. Equal-area, low-hemispheric projection of 10 randomized fault data. Fault dip directions were sampled at random from a range of 0–360°, whereas fault dip angles were from a range of 0–90°. See the caption of Fig. 1 for more explanation.

The procedure used in this section can be described as follows:

(1) assign values to the controlling stress and measurement error,
(2) determine the attitudes of fault striations in the fault planes under the assigned stress,
(3) take each of the options to assign measurement errors to fault/slip data, and estimate the stress from the data with the measurement errors through using the method of Shan et al. (2003), and
(4) calculate the parameters for dispersion of datum vectors and for similarity between the estimated and the controlling stresses.

4.3. Results

Results from the above calculations are shown in Figs. 4–7. As shown in Fig. 4, for a prescribed stress ratio, the root mean square cosine appears generally smaller when due to a small measurement error than that when due to a large error. The maximum, minimum and average values increase with increase of the measurement error, indicating that the root mean square cosine becomes more dispersed when larger measurement errors are added. For a certain error, the root mean square cosine becomes more dispersed when a larger stress ratio is considered. For example, in the case of a measurement error being 8.0°, root mean square cosine has an average value of 0.433 for a stress ratio of 0.0, and of 0.799 for a stress ratio of 1.0. The larger the stress ratio, the more dispersed datum vectors tend to be in the space. This is consistent with the previous conclusion, which states that datum vector can be

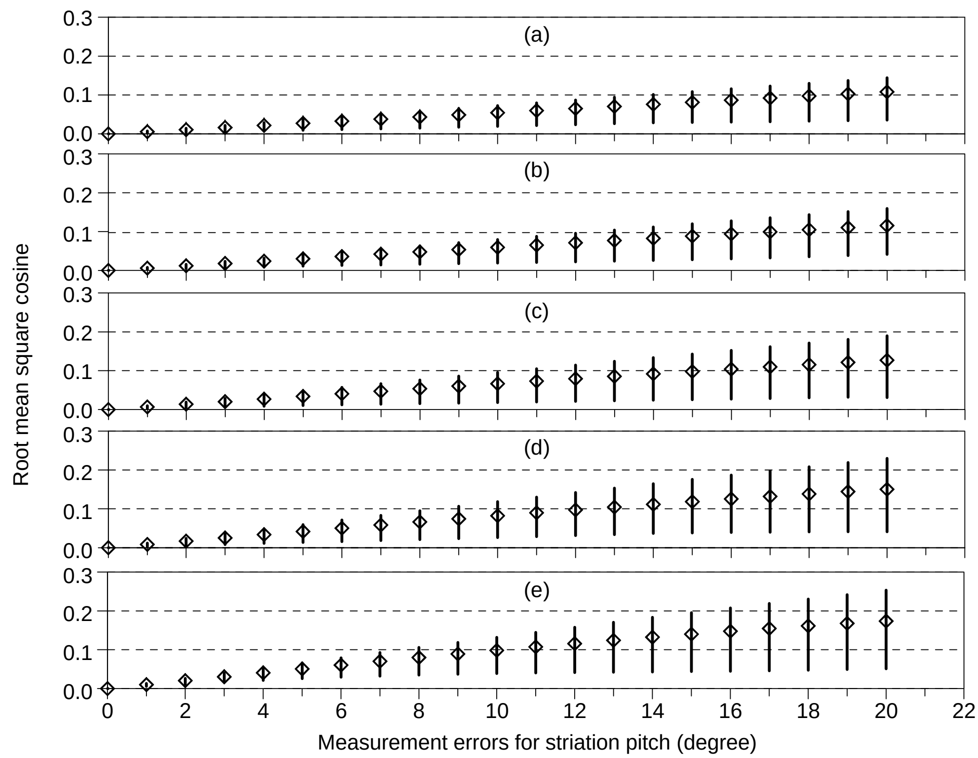

Fig. 4. Root mean square cosines due to different stress ratios of 0.0 (a), 0.25 (b), 0.5 (c), 0.75 (d) and 1.0 (e). The range from the minimum to the maximum (thick line) and average (small diamond) are displayed at each individual measurement error for a given stress ratio.

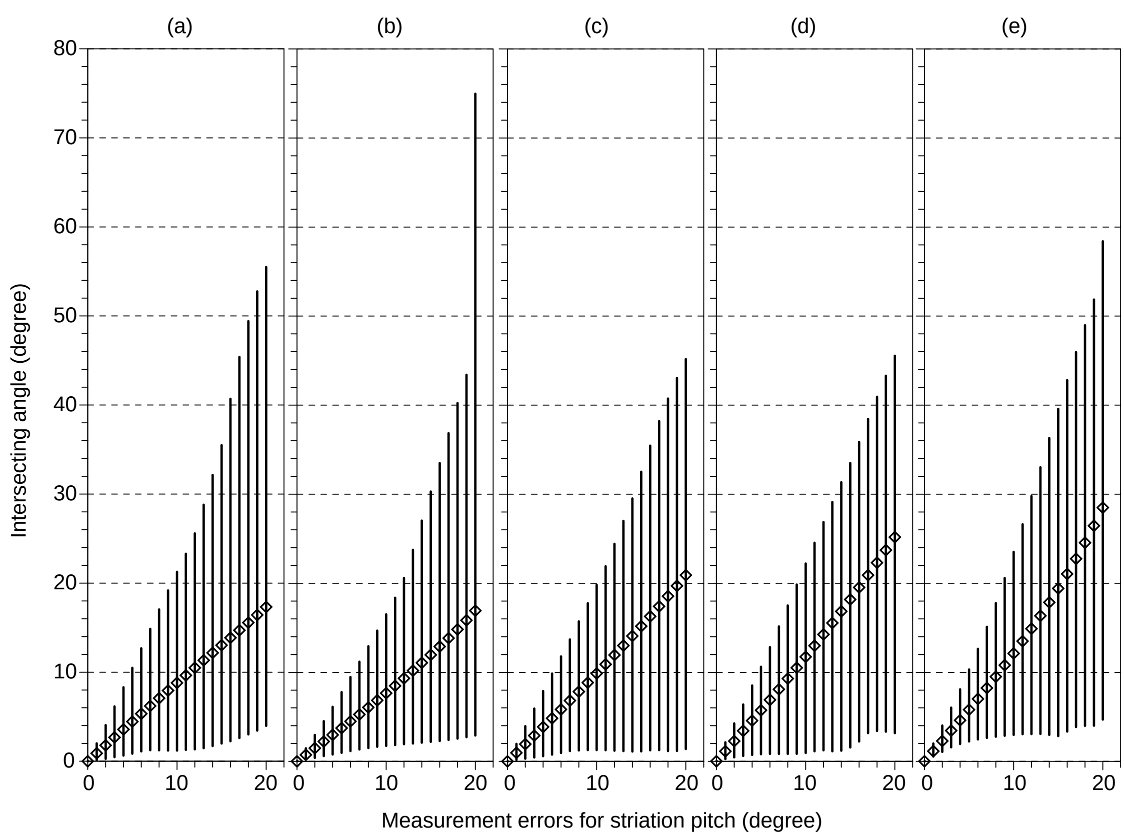

Fig. 5. Intersecting angles between the controlling and the estimated stress vectors due to stress ratios of 0.0 (a), 0.25 (b), 0.5 (c), 0.75 (d) and 1.0 (e). The range from the minimum to the maximum (thick line) and average (small diamond) are displayed at each individual measurement error for a given stress ratio.

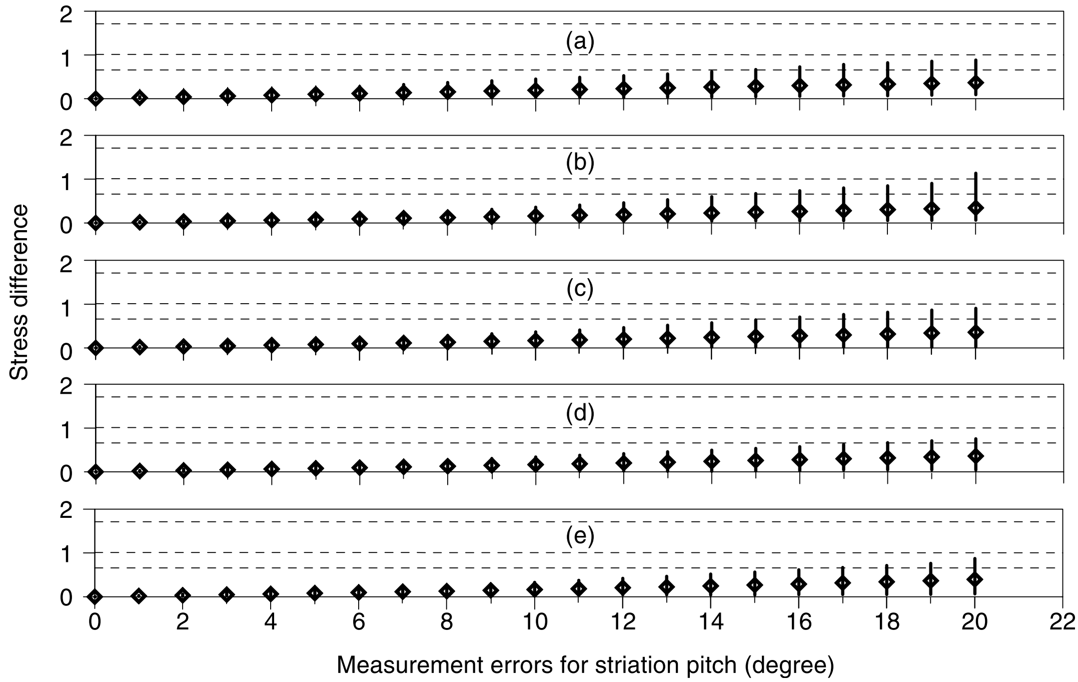

Fig. 6. Differences between the controlling stress and the estimated stress due to different stress ratios of 0.0 (a), 0.25 (b), 0.5 (c), 0.75 (d) and 1.0 (e). The range from the minimum to the maximum (thick line) and average (small diamond) are displayed at each individual measurement error for a given stress ratio. Orife and Lisle's (2003) critical values such as 0.66, 1.01 and 1.71 are shown as dashed lines. See the text for more explanation.

increasingly deviated with increase in the assigned stress ratio. Therefore, the dispersion of datum vectors is affected not only by measurement error, but also by fault orientations (Fig. 3) respective to the controlling stress.

Similarly, the intersecting angle between the controlled and the estimated stress vectors (Fig. 5) is generally smaller when due to a small measurement error than that due to a large error. Both the maximum and the average values increase with increase in the measurement error. The minimum has a strong tendency of increasing with the increase of the measurement error, in spite of some fluctuation(s). The average intersecting angle for a given measurement error also tends to increase with the increase of the assigned stress ratio. An exception to this can be seen in Fig. 5b, where the average values appear smaller in most or all cases than those for a different stress ratio. We believe that, for these instances, the exception can be only explained by the more distinctive influence in stress estimation of fault orientation with respect to the controlling stress. However, there exists no such tendency for the maximum value, which varies significantly with the assigned stress ratio. In sum, the fluctuation of the intersecting angle depends mainly upon two factors, the measurement error and fault orientation with respect to the controlling stress. The larger either of the two

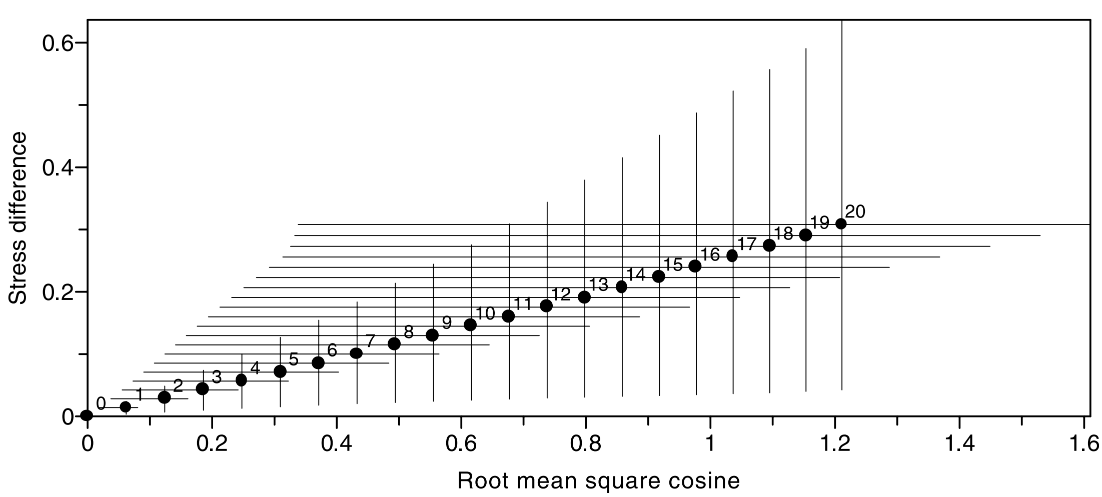

Fig. 7. Relationship between the root mean square cosine and the stress difference due to a stress ratio of 0.0. The range of the former is represented by a horizontal thin line and the range of the latter by a vertical thin line. Both intersect at the averages (small filled circles), near which is the value of corresponding measurement error.

factors is, the greater the intersecting angle tends to be, and the less accurate estimated stress would be. The way they work together is more complicated than we imagined.

Comparison between Figs. 5 and 6 reveals the close similarity in distribution pattern between the stress difference and the intersecting angle. The stress difference is less than 0.66 at an error of less than 15°, indicating a very close similarity between the controlling and the estimated stress tensors. Only in a few cases of a larger measurement error does it exceed 1.01, indicating that the estimated stress tensor is different from the controlling one.

In the light of either the similarity or the intersecting angle, critical values of the stress difference appear to overestimate similarity between controlling and estimated stresses. For example, for a measurement error of 16° and a stress ratio of 1.0, the maximum intersecting angle and the maximum stress difference are 42.812° and 0.615, respectively. One would consider little similarity between the estimated stress and the controlling stress in terms of the large maximal angle, whereas the maximal stress difference indicates they are very similar.

5. Discussion

5.1. Influence of fault orientations

As described above, fault orientations with respect to the controlling stress have an obvious effect on the estimated stress in the presence of a measurement error (Figs. 5 and 6). The misfit between the controlling and the estimated stresses has a strong tendency to increase with the increase of the assigned stress ratio. This is attributed to the increasing possibility of having larger error propagation to a datum vector in reduced sigma space due to a given measurement error and stress ratio (Fig. 2). For homogeneous data sets having small measurement errors, no less than 8° for 10 data in the paper, for instance, fault orientations seem to play such a minor role in affecting the estimated stress, because of the limited error propagation, that they may be neglected in comparison with the measurement error and the simplification associated with fundamental assumptions. However, it is very probable that this minor effect would be aggravated in the case of heterogeneous data relating to the controlling stresses, some or all of them being similar to each other (Shan et al., 2003).

5.2. Accuracy of estimated stress

As shown in Figs. 4–6, the stress difference has something to do with the root mean square cosine. The smaller the root mean square cosine, the smaller the stress difference tends to be. Both have ranges increasing with increase in measurement errors (Fig. 7). For a value of 10° measurement error, and the root mean square cosine of 0.1900–0.7254, the difference is in a range of 0.9319–0.9998, indicating the accuracy of estimated stress. The measurement error, although somewhat large because a smaller one can be guaranteed by careful measurement at most outcrops, still has little role in affecting the accuracy of estimated stress. In spite of the simplification that all artificial data sets used (Fig. 3) are affected only by measurement errors, we believe this approach might be of some value in implying the accuracy of stress estimated from real fault/slip data. For a set of homogeneous data having a small measurement error, less than 10° for instance, we would not like to attribute a large value of the root mean cosine to the error, but to other influences such as heterogeneity of fault/slip data and deviation from assumptions. In this case, we are most likely to have an accurate estimate of stress if the value is small. For carefully measured fault slip data, the measurement error is well controlled, so that its effect on estimated stress would be minor, compared with the effect of other influences.

6. Conclusions

In this paper, numerous sets of homogeneous fault/slip data were generated under varying extensional stress and modified with varying measurement errors for the striation pitch. They were used to investigate error propagation to a datum vector in the reduced sigma space and to examine the accuracy of estimated stress through applying Shan et al.'s (2003) method to the fault/slip data. For this purpose, we performed a vast number of numerical experiments with particular parameters, from which major conclusions have been drawn as follows:

(1) For any given measurement error, the error propagation to a datum vector is affected by the controlling stress (i.e. principal directions and stress ratio) and fault orientation (i.e. dip direction and dip angle). The deviation is approximately of the same order of magnitude as the measurement error itself. It reaches the minimum where the fault dip direction is parallel to the intermediate principal stress. This suggests a greater possibility of an accurately estimated stress as measured faults dip more towards the intermediate principal stress.
(2) For a given stress ratio, both the dispersion of datum vectors (measured by the root mean square cosine) and the misfit between estimated and controlling stresses (measured by the similarity and by the stress difference) increase with increase in measurement error.
(3) Apart from measurement errors and deviation from fundamental assumptions, the orientation of a fault plane relative to the controlling stress is a third influence on the estimated stress. When a measurement error is added to corresponding fault/slip data, the misfit between the controlling and the estimated stresses has a strong tendency to increase with the increase of the assigned stress ratio. However, this influence is minor compared with the influence of the measurement errors.
(4) For the 10 fault/slip data addressed in the paper, the measurement error has an apparent effect in estimated stress only if it is greater than 10°. Below this limit, we always have accurately estimated stress. As a smaller measurement error can be guaranteed by careful measurement at a majority of outcrops, this implies the limited

effect of the measurement error for homogeneous fault slip data that are carefully measured.

Acknowledgements

This was supported by Project MSGL0405-3 from Laboratory of Marginal See Geology, Chinese Academy of Sciences, and by the Hundred Talent Program of the Chinese Academy of Sciences (KZCX0543081001). Dr N. Fry at Cardiff University checked the written English of the paper. Two anonymous referees reviewed the paper and made numerous modifications to it.

References

Angelier, J., 1979. Determination of the mean principal directions of stresses for a given fault population. Tectonophysics 56, T17–T26.

Angelier, J., 1984. Tectonic analysis of fault slip data sets. Journal Geophysical Research B89, 5835–5848.

Angelier, J., 1994. Fault slip analysis and palaeostress construction. In: Hancock, P.L. (Ed.), Continental Deformation. Pergamon Press, Oxford, pp. 53–100.

Armijo, R., Carey, E., Cisternas, A., 1982. The inverse problem in microtectonics and separation of tectonic phase. Tectonophysics 82, 145–160.

Day, S.M., Yu, G., Wald, D.J., 1998. Dynamic stress changes during earthquake rupture. Bulletin of the Seismologic Society of America 88, 512–522.

Etchecopar, A., Vasseur, G., Daignieres, M., 1981. An inverse problem in microtectonics for the determination of stress tensors from fault striation analysis. Journal of Structural Geology 3, 51–65.

Fleischmann, K.H., Nemcok, M., 1991. Paleostress inversion of fault/slip data using the shear stress solution of Means (1989). Tectonophysics 196, 195–202.

Fry, N., 1999. Striated faults: visual appreciation of their constraint on possible palaeostress tensors. Journal of Structural Geology 21, 7–22.

Fry, N., 2001. Stress space: striated faults, deformation twins, and their constraints on palaeostress. Journal of Structural Geology 23, 1–9.

Gutscher, M.A., Kukowski, N., Malavieille, J., Lallemand, S., 1996. Cyclical behavior of thrust wedges: insights from high basal friction sandbox experiments. Geology 24, 135–138.

Hardcastle, K.C., Hills, L.S., 1991. Brute3 and Select: Quickbasic 4 programs for determination of stress tensor configurations and separation of heterogeneous. Computer & Geosciences 17, 23–43.

Huang, Q., 1988. Computer-based method to separate heterogeneous sets of fault-slip data into subsets. Journal of Structural Geology 10, 297–299.

Kleinspehn, K., Pershing, J., Teyssier, C., 1989. Palaeostress stratigraphy: a new technique for analyzing tectonic control on sedimentary-basin subsidence. Geology 17, 253–257.

Koyi, H., 1995. Mode of internal deformation in sand wedges. Journal of Structural Geology 17, 293–300.

Liesa, C.L., Lisle, R.J., 2004. Reliability of methods to separate stress tensors from heterogeneous fault-slip data. Journal of Structural Geology 26, 559–572.

Lisle, R.J., Orife, T., Arlegui, L., 2001. A stress inversion method requiring only fault slip sense. Journal of Geophysical Research 106, 2281–2289.

Mitra, S., 1987. Regional variations in deformation mechanisms and structural styles in the central Appalachian orogenic belt. Geological Society of America Bulletin 98, 569–590.

Nemcok, M., Lisle, R.J., 1995. A stress inversion procedure for polyphase fault/slip data sets. Journal of Structural Geology 17, 1445–1453.

Nemcok, M., Kovac, D., Lisle, R.J., 1999. Stress inversion procedure for polyphase calcite twin and fault/slip data sets. Journal of Structural Geology 21, 597–611.

Orife, T., Lisle, R.J., 2003. Numerical processing of palaeostress results. Journal of Structural Geology 25, 949–957.

Price, R.A., 1988. The mechanical paradox of large thrusts. Geological Society of America Bulletin 100, 1898–1908.

Ramsay, J.G., Lisle, R.J., 2000. Modern Structural Geology, Vol. 3. Continuum Mechanics for Structural Geologists. Academic Press, London. 360pp.

Shan, Y., Fry, N., 2005. A hierarchical cluster approach for forward separation of heterogeneous fault/slip data into subsets. Journal of Structural Geology 27, 929–936.

Shan, Y., Suen, H., Lin, G., 2003. Separation of polyphase fault/slip data: an objective-function algorithm based on hard division. Journal of Structural Geology 25, 829–840.

Shan, Y., Li, Z., Lin, G., Li, J., 2004a. A simple stress inversion of fault/slip data assuming Andersonian stress state. Journal of Geophysical Research 109, B04408. doi:10.1029/2003JB002770.

Shan, Y., Li, Z., Lin, G., 2004b. An inverse method to determine the optimal stress from imperfect fault data. Tectonophysics 387, 205–215.

Shan, Y., Lin, G., Li, Z., 2004c. A stress inversion procedure for automatic recognition of polyphase fault/slip data sets. Journal of Structural Geology 26, 919–925.

Simón-Gómez, J.L., 1986. Analysis of a gradual change in stress regime: example from the eastern Iberian Chain. Tectonophysics 124, 37–53.

Xu, P., 2004. Determination of regional stress tensors from fault-slip data. Geophysical Journal International 157, 1316–1330.

Yamaji, A., 2000. The multiple inverse method: a new technique to separate stresses from heterogeneous fault-slip data. Journal of Structural Geology 22, 441–452.